Egypt. J. Chem. **Vol. 65**, No 4. pp. 351-361 (2022)

Egyptian Journal of Chemistry

http://ejchem.journals.ekb.eg/

Eco-Friendly Roselle (Hibiscus Sabdariffa) Leaf Extract as Naturally Corrosion Inhibitor for Cu-Zn Alloy in 1M HNO_3

Seham Shahen[a] , Amal M. Abdel-karim,[b]* and Ghalia A. Gaber[a]

[a] *Department of Chemistry, Faculty of Science (Girls), Al-Azhar University, P.O. Box: 11754, Yousef Abbas Str., Nasr City, Cairo, Egypt*

[b] *Physical Chemistry Department, National Research Centre, 33 El Bohouth St. (El-Tahrir St. former) Dokki, Giza, P.O.12622 Egypt*

Abstract

The eco-friendly compounds especially plant extracts have emerged as great green corrosion inhibitors for metals and alloys. The inhibiting impact of the Roselle extract on Cu-Zn alloy in 1M HNO_3 solution was studied by weight loss, electrochemical impedance spectroscopy (EIS), and potentiodynamic polarization (PDP). It was found that Roselle extract acts as a mixed-type corrosion inhibitor for Cu-Zn alloy in an acid solution. The corrosion rate decreases with increasing the extract concentration and increases with raising the temperature. The formation of a protecting film on the Cu-Zn alloy surface with the presence of Roselle extract was shown and confirmed by scanning electron microscopy (SEM), and energy-dispersive X-ray (EDX). The high inhibition efficiency of 94.89 % was recorded for 80% extract solution. There are good agreements between the results from all techniques.

Keywords: Cu-Zn alloy; Nitric acid; Corrosion inhibition; Roselle (Hibiscus Sabdariffa) extract

1. Introduction

Copper has great properties leading to a wide scope of uses. It is utilized in hardware, for the creation of wires, cylinders, and furthermore to form alloys [1-4]. Copper is effortlessly joined with numerous metals as zinc created brass alloy. The brass is used in the valves, distillation plants, cooling systems, and condenser systems. Cu-Zn alloy is more earnest and strong and has a higher corrosion obstruction. Be that as it may, their show in corrosive media makes issues of corrosion [5-8]. At the point when the brass alloys contain over 15% zinc they are influenced by broad consumption harm in destructive conditions yet additionally by the dezincification process including the disintegration of zinc, leaving an elastic mass of Cu on the composite surface [9]. The efficiency of natural inhibitors is for the most part credited to the heteroatom, for example, nitrogen, oxygen, sulfur, and π bonds, which go about as a functioning group for adsorption on the surface [10]. Utilizing mixes containing in their atomic

*Corresponding author e-mail: amalabdelkarim720@gmail.com
Received date 27 August 2021; Revised date 19 September 2021; Accepted date 20 October 2021
DOI: 10.21608/EJCHEM.2021.92917.4392

structures N, P, and S may prompt the creation of exceptionally poisonous mixes influencing both people and nature. As for the different ecological impediments, consideration has been centered on exploring some natural corrosion inhibitors identified as “green corrosion inhibitors" they are cheap, available, and a renewable source. This can work with higher efficiency and lower poisonous [11-15]. As regular natural inhibitors, plant extracts have high efficiency. The use of pectin eco-friendly natural polymer as a corrosion inhibitor on mild steel in hydrochloric media gives maximum inhibition efficiency of 91.5% and 93.9% obtained using 1 g/l of both acid and enzyme extracted pectin respectively [16].

Roselle (Hibiscus Sabdarriffa) is a natural plant developed in Egypt as a warm nation and is rich particularly in proteins, and dietary fiber [17]. Dried flowers contain flavonoids, polyphenolic acids, anthocyanins sabdaretine, and hibiscetine. The significant red color reported as hibiscus, has been identified as delphinidin, delphinidin-3-monoglucoside, and cyaniding 3-monoglucoside [18]. Roselle is related to customary medication and is broadly used to hinder the development of kidney stones, hypertension, and liver issues [19-22]. In addition to having the above the choice of Roselle as a corrosion inhibitor is due to its abundant, eco-friendly, and inexpensive plant. Emeka E. studied the inhibiting action of the extract of Roselle on mild steel corrosion using a gasometric technique in HCl and H_2SO_4 solutions. He found that the extract suppressed the corrosion reaction in 1 M H_2SO_4 slightly higher than 2M HCl [23]. The adsorbed protective film of Roselle extract was formed in 5 M HCl to inhibit the dissolution of mild steel by adding different concentrations of aqueous extract of the Hibiscus Sabdariffa plant as an eco-friendly inhibitor [24]. The use of Roselle as an inhibitor for pure Al in 0.5 M H_2SO_4 at different temperatures has been evaluated using different tests such as gravimetric, potentiodynamic polarization, and EIS measurements. It was found that the inhibition efficiency improved with extract concentration and decreased with temperature [25].

The purpose of this work is to examine the corrosion inhibition of Cu-Zn alloy using Roselle extract in the 1M HNO_3 solution. Different techniques were used as weight reduction, PDP, EIS, adsorption isotherm, and surface morphological studies. The thermodynamic and activation parameters for the adsorption process were calculated and discussed.

1. Experimental

2.1. Preparation of plant extracts

Fresh parts of Roselle were obtained from Isis Organic, Egypt. The red calyces of Roselle were cut, washed with distilled H_2O, dried, ground into powder, and weighed. Using a reflux process, stock solution extraction was carried out. The extract was resulted by Soxhlet extractor using two distinct solvents with polarities, at temperature 60-80 ^oC petroleum ether was used followed by methanol to obtain the fraction of two solvent that was evaporated with butanol to provide the fraction of butanol that was evaporated to include a solid extract prepared for application. Fig.1 shows the photo-image of Rosella and the important functional group in flavonoids structure.

2.2. Materials and solutions

Cu-Zn alloy with the following composition: Cu 84 wt. % and Zn 16 wt. % the pieces were polished with silicon carbide paper from 600 to 1200 grades to a metallic shine and rinsed with acetone and distilled water. Dilution is of analytical reagent grade 67.5 percent HNO_3 with distilled H_2O to prepared 1M of the aggressive solution used. The stock solution of Roselle extracts was used to prepare the necessary concentrations (10-80%) by dilution

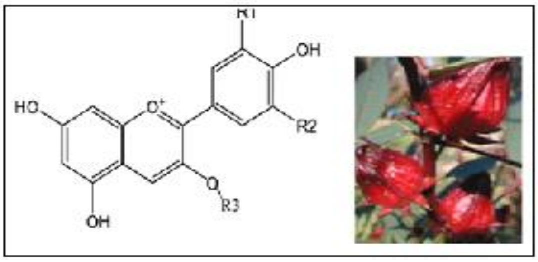

Fig. 1 The photo image of Rosella and important functional groups in general structure of flavonoids

2.3. Weight loss estimations

2.3.1. Effect of Roselle extracts

Cu-Zn alloy polished pieces of 2.2x 2.0x 0.2 cm were immersed in 100 ml of 1 M HNO_3 solutions with and without different Roselle extracts (10, 30, 50, 70, and 80%) at room temperature for 6 days. After specific periods, the Cu-Zn alloy was removed, washed with distilled water then dried and weighed. The inhibition efficiency (IE) and corrosion rate (CR) are determined by:

$$IE\% = \frac{w_2 - w_1}{w_2} x100 \qquad (1)$$

Where, W_1 and W_2 are the weight loss of the Cu-Zn alloy in the presence and the absence of extract respectively.

$$\text{The surface coverage } (\theta) = \frac{IE}{100} \qquad (2)$$

The corrosion rate (CR) was determined from

$$CR = \frac{(\Delta m)}{S.t} \qquad (3)$$

Where, Δm (mg) is the weight before and after immersion in the tested solution, S is the area of the Cu-Zn alloy specimen (cm^2) and t is the exposure time (h).

2.3.2. Effect of temperature

The variation in the corrosion rate with the temperature in 1 M HNO_3 was determined during 2 h of immersion, both in the absence and presence of Roselle extract. Gravimetric trials were performed at 303–343 K. To compute activation thermodynamic boundaries of the corrosion process, Arrhenius Eq. (4) and progress state Eq. (5) were utilized [26]:

$$C_R = A\ exp\left(\frac{E_a}{RT}\right) \qquad (4)$$

$$CR = \frac{RT}{Nh} exp \frac{\Delta S_a^o}{R} ex\left(-\frac{\Delta H_a^0}{RT}\right) \qquad (5)$$

Where E°_a is the actual activation energy, R is the gas constant, A is the pre-exponential factor of Arrhenius, h is the constant of Plank, N is Avogadro, ΔS°_a is the entropy, and ΔH°_a is the enthalpy.

2.4. Adsorption isotherm

Additional details about the features of the compounds tested can be produced by the adsorption isotherm. From the weight reduction estimates, the degree of surface coverage values (θ) for investigated inhibitor (Roselle extract) calculated by eq. 2.

2.5. Electrochemical measurements

All the electrochemical studies were performed using three-electrode cell Autolab Potentiostat/ Galvanostat 302N. Nova 1.11 software installed on a computer was used for fitting data. Cu-Zn alloy (1x 2x 0.02 cm) is the working electrode with an exposed area of 1 cm^2, Ag/AgCl as the reference electrode, and pt wire as the counter electrode. Polarization curves were obtained by changing the electrode potential from -1.2 to 0.6V from the open circuit potential (OCP) with a 1 mVs^{-1} scan rate. The corrosion parameters were obtained.

The impedance method was done at OCP with a sinusoidal excitation signal of 10 mV in the frequency range 0.01Hz to 100 kHz. Analyze the data obtained from the EIS curves that fit specific circuits and give some parameter as charge transfer resistance, double-layer capacitance, and thickness of the adsorbed film.

2.6. Surface analysis

The specimens used were immersed in 1 M HNO_3 With and without 80 percent extracts at room temperature for 24 h. The surface morphology was performed using a scanning electron microscope (JOEL 840, Japan) with EDX. The specimens were gently washed with distilled H_2O, carefully dried, and examined without additional treatment.

3. Results and Discussion

3.1. The effect of Roselle extracts concentration

IE % and CR values achieved by the technique of weight loss at different Roselle extract concentrations at 298 K are condensed in Table 1 and Fig. 2 and 3. As seen in presence of Roselle extract, the loss in weight of the alloy specimens is decreased. The loss in weight becomes higher with increasing the concentration of Roselle extract. This action may be attributed to a competitive step, including passive film healing by the Roselle extract and passive film damage by the aggressive ions. The outcomes revealed that the corrosion rate of Cu-Zn alloy diminished consistently with expanding the extract concentration, i.e., the consumption of Cu-Zn alloy is hindered by Roselle extract. IE% increments pointedly with increments in extract concentration arriving at the most extreme estimation of 97.59% in presence of 80% of the extract. This conduct could be clarified by the adsorption of segments of the extract on the surface of Cu-Zn alloy bringing about the hinder of the dissolution and protecting the surface in the corrosive medium [7].

Thusly, we can infer that the Roselle Extract is a good inhibitor for Cu-Zn alloy in 1 M HNO_3.

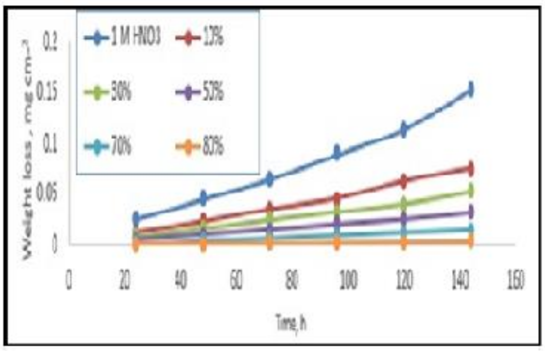

Fig. 2 Weight loss-Time curves for Cu-Zn alloy in 1M HNO_3 acid solution with and without Roselle extract at 298K

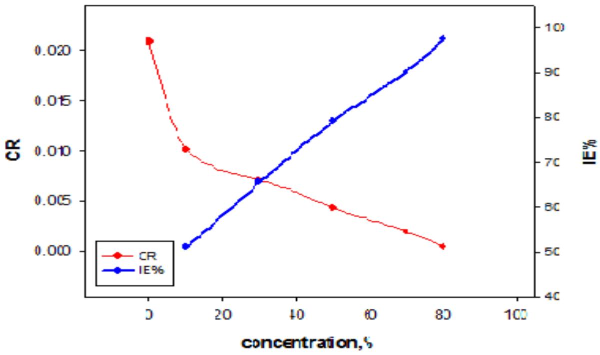

Fig.3 The corrosion rate (CR) and inhibition efficiency (IE) of Cu-Zn alloy in 1M HNO_3 as a function of Roselle Extract concentration at 298K.

Table 1: Results of weight loss of Cu-Zn alloy in 1M HNO_3 With and without different concentrations of Roselle extract at 298 K.

Inhibitor	Conc. (%)	CR (mpy)	Coverage surface (θ)	Efficiency (IE %)
Blank	0	0.0209	-	-
Roselle Extract	10	0.0102	0.512	51.23
	30	0.0071	0.657	65.73
	50	0.0043	0.792	79.25
	70	0.0020	0.902	90.24
	80	0.0005	0.975	97.59

3.2. Adsorption isotherm

The surface coverage (θ) calculated from the weight reduction technique listed in Table 1 was graphically tested for fitting a suitable adsorption isotherm. Fig. 4 shows the plot of C/θ versus C (extract concentration) which is typical of the Langmuir adsorption isotherm [23], which expressed by:

$$\left(\frac{C}{\theta}\right) = \left(\frac{1}{K_{ads}}\right) + C \qquad (6)$$

Where, K_{ads} is the adsorption equilibrium constant. A linear plot was obtained with R^2 = 0.97508 and a slope about unity 0.8819. K_{ads} was 6.567 calculated from the intercept of the straight line of the isotherm.

The standard free energy (ΔG_{ads}) can be calculated by the following Equation [27]:

$$K_{ads} = \frac{1}{55.5} \exp\left(\frac{-\Delta G_{ads}}{RT}\right) \qquad (7)$$

Where the value 55.5 is the molar concentration of H_2O, R is the gas constant, and T is the temperature.

It is found that the value of ΔG_{ads} is -14.614 $kJmol^{-1}$. This negative value points to that the adsorption process is spontaneous. In addition, the values of ΔG_{ads} at or below -20 kJ mol^{-1} are consistent with the electrostatic interaction between both charged metal and molecules (physisorption), while the values of ΔG_{ads} at or below -40 kJ mol^{-1} include the charge transfer or sharing from the inhibitor molecules to the metal surface to form a co-ordinate bond type (chemisorption) [28]. The calculated value of ΔG_{ads} is less negative than -20 kJ mol^{-1} demonstrating that physisorption is typical of the adsorption process of the investigated Roselle extract on Cu-Zn alloy in 1 M HNO_3. The mode of adsorption observed may be because there are different chemical compounds found in the investigated inhibitor, some of which can be chemically adsorbed and others physically adsorbed [29].

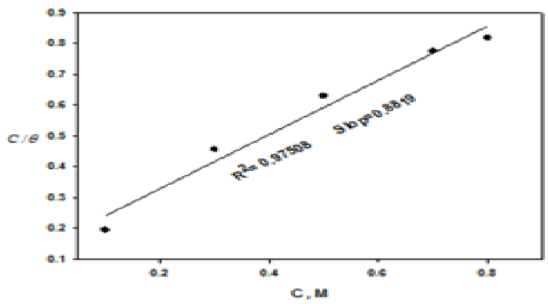

Fig. 4 The plot of C/θ vs. C for Cu-Zn alloy derived from weight reduction data in 1M HNO_3 with and without Roselle extract.

3.3. Effect of temperature

The impact of temperature on the corrosion of Cu-Zn alloy in 1 M HNO_3 containing Roselle Extract at 80 % was studied in the temperature range from 303 to 343 K utilizing weight reduction estimations at 2 h. The information on CR and IE % collected were introduced in Table 2 and Fig. 5. A review of these outcomes uncovers that the CR increases with temperature both in uninhibited and inhibited solutions particularly going up more quickly without inhibitor. This outcome shows that the occurrence of the inhibitor prompts a reduction of the corrosion rate. Additionally, we note that IE relies upon the temperature and diminishes with the ascent of temperature from 303 to 343 K. The efficiency (IE) arrived at a high estimation of 92.5% in 1 M HNO_3 at 303 K, which speaks to the amazing inhibitive capacity of Roselle extract. The decline in hindrance productivity with increment in temperature might be credited to the expanded desorption of inhibitor from the surface. These indicate that the process of adsorption of the Roselle inhibitor on the alloy surface is physical adsorption [30]. The presence of π-orbital and unshared electrons of heteroatom blocked the active sites. These mixes contain distinctive hetero molecules and fused benzene rings which improve the inhibition efficiency.

Table 2: Corrosion parameters derived from weight loss of Cu-Zn alloy in 1 M HNO_3 containing 80% Roselle extract at different temperatures.

Temp. (K)	CR Of Blank (mpy)	CR With inhibitor (mpy)	IE %
303	0.1966	0.0147	92.5
313	0.4424	0.0884	80.00
323	0.8947	0.2949	67.03
333	1.789	0.7866	56.04
343	3.244	1.671	48.48

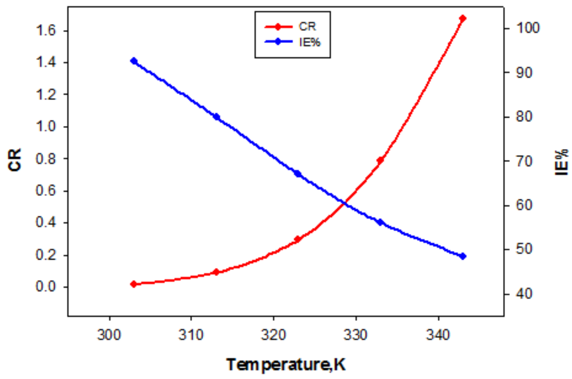

Fig. 5 Influence of temperature on the CR and IE% of Cu-Zn alloy in 1M HNO_3 in the presence of 0% of Roselle extract as a function of temperatures

Fig. 6 represents the Arrhenius plot of ln (CR) versus (1/T) for Cu-Zn alloy in 1M HNO_3 in the absence and presence of 80% of Roselle extract. The slope of the straight lines is equal to $-E_a/R$. The values of activation energy (E_a) with and without the extract were calculated and are equal to 60.538 and 101.132 kJ mol^{-1}, respectively. It is noticed that the value of E_a of the inhibited solution is higher than the uninhibited; due to the formation of the adsorbed film on the surface with the increasing thickness that decreases the dissolution of Cu-Zn alloy [31, 32].

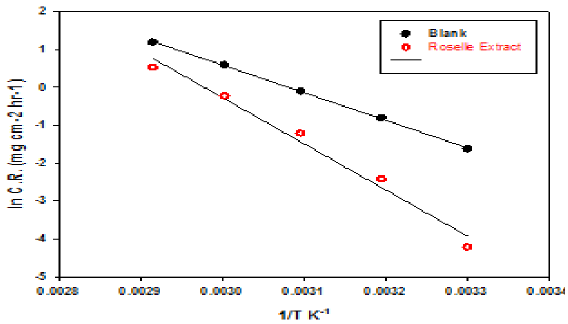

Fig. 6 Arrhenius plot ln CR and 1/T for Cu-Zn alloy in 1M HNO_3 in the absence and presence of 80% of Rosella extract.

The values of heat of adsorption Q_{ads} of the investigated extract on Cu-Zn alloy were obtained using Eq. 8 [33].

$$\log\left(\frac{\theta}{1-\theta}\right) = \log A + \log k - \frac{Q_{ads}}{2.303R}\left(\frac{1}{T}\right) \qquad (8)$$

Where, T is the absolute temperature, θ is the surface coverage, and A is the independent constant.

The heat of adsorption value was obtained from the slope ($- Q_{ads}$ /2.303 R) of a plot of log (θ/1-θ) against (1/T) for the Cu-Zn alloy in presence of Rosella extract is shown in Fig. 7. The heat of adsorption is equal to (-54.759 kJ mol^{-1}) for Cu-Zn alloy in 1M HNO_3 in the presence of 80% of Roselle extract. The value of Q_{ads} is negative; indicating the exothermal nature of the dissolution process of the Cu- Zn alloy [31]. The apparent enthalpy ΔH_{ads} and the entropy ΔS_{ads} values were obtained using Eq. 5. Plots of ln (CR/T) versus 1/T for Cu-Zn alloy in 1M HNO_3 in the presence of 80% of Roselle extract are shown in Fig.8, the linear relation with a slope of (-ΔH/R) and intercept of (ln (R/Nh)+ΔS/ R) where the enthalpy and entropy was estimated respectively. The ΔH are 57.864 and 98.457 kJ mol^{-1} for an uninhibited and inhibited solution, respectively. ΔH values are positive, indicating that the corrosion process is endothermic and therefore a slow dissolution of Cu-Zn alloys [34].

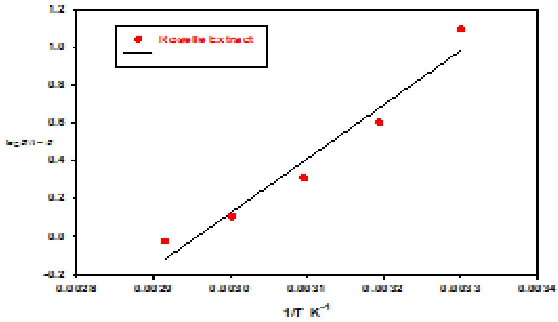

Fig. 7 A plot of log (θ/ 1-θ) against 1/T for Cu-Zn alloy in 1M HNO_3 in the absence and presence of 80% of Rosella extract

The entropy in the absence and presence of 80% of the extract is -67.410 and - 47.203 k J mol^{-1}, respectively. The negative values of ΔS_{ads} mean a decrease in disorder occurred on the passage from reactants (Roselle extract) to the activated complex with the metal [33].

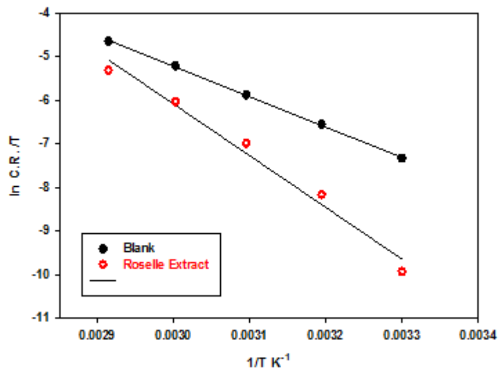

Fig. 8 A plot of ln CR/T vs. 1/T curves for Cu-Zn alloy in 1M HNO_3 in the absence and presence of 80% of Rosella extract.

3.4. Electrochemical impedance spectroscopy (EIS)

Nyquist and bode curves of Cu-Zn alloy in inhibited and uninhibited acid solutions containing different Roselle concentrations are presented in Fig.8. Nyquist spectra consist of the depressed capacitive loop (charge transfer process) and Warburg loop (diffusion process). The diameter of the Nyquist loop increase with increasing extract concentration, indicating the high inhibition of Cu-Zn alloy corrosion.

Fig. 9 shows the equivalent circuit used to analyze the impedance spectra. Excellent fitting was obtained for all experimental data. Warburg impedance (W) represents the diffusion process which decreases with the increase of inhibitor indicating that the diffusion process was retarded by adsorption

$$C_{dl} = \left(\frac{1}{Y_o(j\omega)^n}\right) \qquad (9)$$

Where, y_o is the CPE magnitude of, ω is the frequency at which the maximum imaginary part of the impedance.

Impedance parameter listed in Table 3, it is observed that the resistance values increase and C_{dl} decrease with the increase an extract concentration. That decrease in the C_{dl} value due to an increase in the thickness of the double layer (d), indicated that the Roselle extracts inhibit the corrosion of Cu-Zn alloy by adsorption on the metal/acid interface [35].

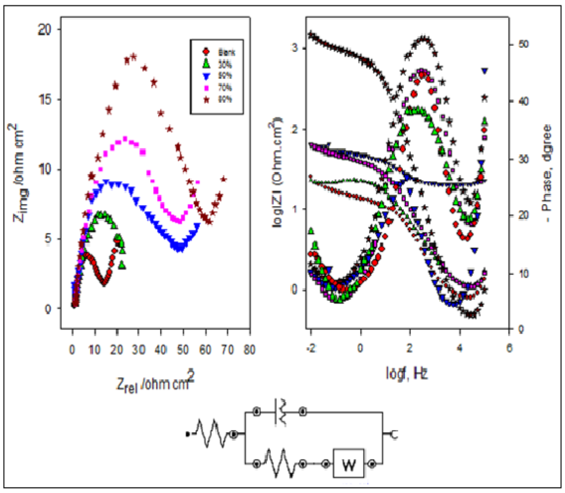

Fig. 9 Nequist, Pod and Phase plots of Cu-Zn alloy with and without different concentration of Rosella extract in 1M HNO_3.

Table (3) EIS parameters of Cu-Zn alloy in 1M HNO_3 with and without different concentration of Roselle extract

Conc.	*Rs*(Ω)	*Q₁* (μF cm^{-2})	*n*	*R₂* (Ωcm²)	*W* (μF cm²)	*d* (μF-1 cm²)
Blank	0.784	2.41x10^{-3}	0.666	12.00	0.346	0.00041
30%	0.950	2.31x10^{-3}	0.621	20.25	0.747	0.00043
50%	0.834	1.56x10^{-3}	0.635	44.59	0.203	0.00064
70%	1.800	1.30x10^{-3}	0.617	43.52	0.197	0.00076
80%	1.002	9.51x10^{-4}	0.670	57.76	0.188	0.001

3.5. Potentiodynamic polarization measurements

Fig.10 represents the effect of Roselle extract on the anodic and cathodic polarization in 1M HNO_3. It is seen that the cathodic branch was affected and the slight effect on the anodic branch led to retard the hydrogen evolution and lowering the Cu-Zn alloy dissolution.

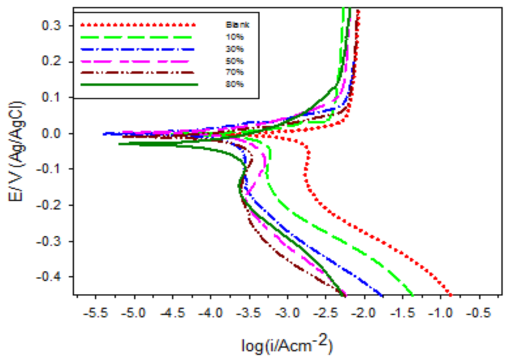

Fig.10 Potentiodynamic polarization curves for Cu-Zn alloy in 1M HNO_3 in the absence and presence of different concentration of Roselle extract

All parameters were tabulated in Table 4 as E_{corr} corrosion potential, I_{corr} corrosion current, R_{pol} polarization resistance, Tafel slope ßa, ßc anodic and cathodic, respectively. The ßa and ßc changed slightly indicating the influence of extract on the kinetics of hydrogen evolution and metal dissolution.

I_{corr} was obtained from the extrapolation of the Tafel lines (anodic and cathodic) to the corrosion potential. The corrosion current density decreases from 7.80x10^{-4} A cm^{-2} of blank to 3.70x10^{-5} A cm^{-2} with 80% extract. The CR of blank is found to be 9.01 mm/y and it is minimized by adding an inhibitor reaching a lower value of 0.45 mm/y at 80% Roselle extract.

The inhibition efficiency was calculated from the polarization study using the following equation:

$$IE\% = [1 - \left(\frac{i_{corr}}{i^{o}_{corr}}\right) x100 \qquad (10)$$

Where, i_{corr} and $i°_{corr}$ are the current densities without and with Roselle extract inhibitor, respectively.

It is found that the IE is equal to 94.89% of the optimum concentration of 80%. This high efficiency value is due to the adsorption of the inhibitor molecules by the active sites as hetero-atoms and aromatic rings. The approximately constant values of ßa indicate that the inhibitor was first adsorbed onto the Cu-Zn alloy surface and impeded by blocking the reaction sites of the alloy surface without affecting the anodic reaction mechanism. The inhibition efficiency calculated from polarization measurements is in good harmony with those obtained from the weight loss method

Table 4: The polarization parameter values for Cu-Zn alloy in 1 M HNO3 with and without Roselle extract.

Conc. %	β_a (mV dec^{-1})	β_c (mVdec^{-1})	I_{corr} (Acm^{-2})	R_P (Ohm. cm^2)	C.R (mm/y)	IE (%)
Blank	0.090	0.038	7.80x10^{-4}	14.86	9.01	------ -
10	0.045	0.142	1.65x10^{-4}	88.98	1.95	78.4
30	0.046	0.056	1.13x10^{-4}	96.56	1.32	85.5
50	0.056	0.107	9.16x10^{-5}	173.78	1.06	88.2
70	0.029	0.068	5.53x10^{-5}	159.44	0.64	92.9
80	0.026	0.046	3.70x10^{-5}	182.34	0.45	94.9

3.6. Scanning Electron Microscopy (SEM)

SEM of the Cu-Zn alloy after immersion for 24 h in 1 M HNO_3 was reported in the absence and presence of 80% Roselle extract. Fig. 11(a) demonstrates the Cu-Zn alloy surface in 1M HNO_3. From this figure, the surface was completely corroded and was covered with high-density pits. The presence of Roselle extract Fig.11 (b) improves the resistance of the surface, shows no pit and the growth of the adsorbed protected layer of the inhibitor blocks the active site of the alloy surface and decreases its contact with aggressive medium revealing a smooth surface and good inhibition.

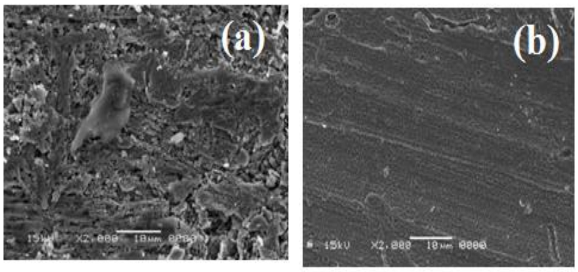

Fig.11 SEM image of Cu-Zn alloy surface after 24 h of immersion in (a) 1 M HNO_3 and (b) 1 M HNO_3 with 80% of extract.

To analyze the composition of the formed film was studied by EDX as shown in Fig. 12. It is seen that in blank solution EDX shows that the Cu, Zn, and Oxygen are present. In presence of the optimal concentration of inhibitor the peak for S, N appeared. Morphology and the EDX of the surface prove the protective film of Roselle extract on the Cu-Zn alloy.

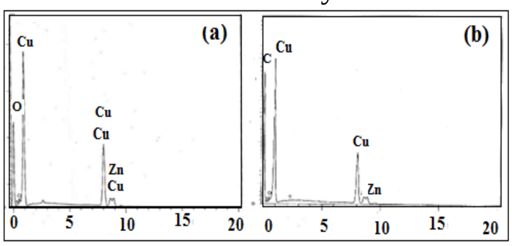

Fig.12. EDX charts of Cu-Zn alloy surface after 24 h of immersion in (a) 1 M HNO_3 and (b) with 80% of Rosella extract at 25°C.

3.7. Mechanism of inhibition

Adsorption of the component of Roselle extract at the Cu-Zn alloy forms protecting layer in 1M HNO_3, and the pace of adsorption is quickened and shields the Cu-Zn alloy surface from aggressive media [36]. Roselle extract contains various organic substances such as flavonoids, ascorbic acid, tannins, amino acids, phenolic mixes, gossypetin, and anthocyanins [37, 38]. It is notable that Cu-Zn surfaces have a positive charge in acidic solutions [39].so it is difficult for the protonated extract concentrate to push toward the positively charged Cu-Zn alloy (H_3O^+/metal interface) because of electrostatic repulsion. While the presence of nitrate ions can generate a negative charge and enhance electrostatic interaction for further adsorption of the protonated inhibitor.

This is in conformity with the results derived from the isothermal adsorption (physisorption). Synergism among NO_3^- and Roselle extract particles improves the inhibition efficiency. Positively charged species (thiamine and anthocyanins) are adsorbed with the negatively charged alloy surface giving rise to a physical adsorption mechanism [40, 41]. In this way, we can infer that the restraint of Cu-Zn alloy consumption by the Roselle extract in 1M HNO_3 is due to the electrostatic interaction which is confirmed by the reduction in efficiency with an ascent temperature.

3. Conclusions

Roselle extract has ended up being a good green inhibitor for the corrosion of Cu-Zn alloy in 1M HNO_3. Weight loss tests show that the corrosion rates were reduced and the inhibition efficiency increments with an increase in the concentration of Roselle extract the most significant efficiency was found 97.59% of 80% extract. The adsorption isotherm of Roselle on Cu-Zn alloy can be clarified by Langmuir isotherm. As indicated by the got estimations of ΔG^o_{ads}, the physisorption was considered. The corrosion rate and corrosion current density decrease while the resistance and the inhibition efficiency increase with increasing the inhibitor concentration. EIS studies indicate that the charge transfer resistance increase with increasing Roselle extract. The outcomes acquired from the SEM method affirmed that a protective layer of red Roselle extract is formed on the metal surface in 1M HNO_3.

Funding

No funding is available.

Declarations

Conflict of interest No conflict exist and the authors declare that they have no conflict of interest

References

1. Motawea M. M., El-Hossiany A. and Fouda A. S., Corrosion Control of Copper in Nitric Acid Solution using Chenopodium Extract, Int. J. Electrochem. Sci., 14, 1372 – 1387 (2019).
2. Souza F.S. De, Giacomelli C., Gonçalves R.S. and Spinelli A., Adsorption behavior of caffeine as a green corrosion inhibitor for copper, Mater. Sci. Eng., 32(8), 2436–2444 (2012).
3. Abd-El-Nabey B.A., Abdel-Gaber A.M., Said Ali M. El., Khamis E. and El-Housseiny S., Inhibitive Action of Cannabis Plant Extract on the Corrosion of Copper in 0.5 M H2SO4, J. Electrochem. Sci., 8, 7124–7137 (2013).
4. Mandour, H. S., Abdel-Karim, A. M., & Fathi, A. M. Inhibition Efficiency of Copper Corrosion in a Neutral Chloride Solution by Barbituric and Thiobarbituric Acids , Portugaliae Electrochimica Acta 39 ,85-103(2021).
5. Fouda A.S. and Abdel Haleemb E., Berry Leaves Extract as Green Effective Corrosion Inhibitor for Cu in Nitric Acid Solutions, Surf. Eng. Appl. Electrochem., 54 (5), 498–507 (2018).
6. Fouda A.S., Rashwan S.M., Darwish M.M.K. and Arman N.M., Corrosion

Inhibition of Zn in a 0.5 M HCl Solution by Ailanthus Altissima Extract, Portugaliae, Electrochim. Acta, 36 (5), 309-323 (2018).
7. Fouda A.S., El-Dossoki F.I., El-Nadr H.A. and El Hussein A., Moringa oleifera plant extract as a copper corrosion inhibitor in binary acid mixture (HNO3 + H3PO4), Zastitamaterijala, 59 (3), 422 -435 (2018).
8. El-Haddad M.N., Chitosan as a green inhibitor for copper corrosion in acidic medium, Int. J. Biol. Macromol., 55, 142-149 (2013).
9. Gualdrón A.F., Becerra E.N., Peña D.Y., Gutiérrez J.C. and Becerra H.Q., Inhibitory effect of Eucalyptus and Lippia Alba essential oils on the corrosion of mild steel in hydrochloric acid, J. Mater. Environ. Sci., 4 (1), 143-158 (2013).
10. Fathi, A. M., Mandour H. and Abdel-Karim, A. M. The Inhibiting Effect of Non Toxic 4-Amino antipyrine and 4,6-Dimethyl-1H-pyrazolo[3,4 b]pyridin-3-mine on Mild steel Corrosion in Sulphuric acid, Int. J. Electrochem. Sci., 11 , 5580 – 5595 (2016).
11. Abdel-karim, A.M., Shahen, S. and Gaber, G. A., 4-Aminobenzenesulfonic acid as Effective Corrosion Inhibitor for carbon steel in hydrochloric acid. Egyptian Journal of Chemistry, 64(2), 825-834(2021).
12. Abdallah Y.M., Hassan H.M., Shalabi K. and Fouda A.S., Effects of Arctostaphylosuva-ursi Extract as Green Corrosion Inhibitor for Cu10Ni Alloy in 1 M HNO3, Int. J. Electrochem. Sci., 9, 5073–5091 (2014).
13. Fouda A.S., Shalabi K., Elewady G.Y. and Merayyed H.F., Chalcone Derivatives as Corrosion Inhibitors for Carbon Steel in 1 M HCl Solutions, Int. J. Electrochem. Sci., 9, 7038–7058 (2014).
14. Al-Amiery A.A., Kassim F.A.B., Kadhum A.A.H. and Mohamad A.B., Synthesis and characterization of a novel eco-friendly corrosion inhibition for mild steel in 1 M hydrochloric acid, Sci. Rep., 6: 19890 (2016).
15. Saadouni M., Larouj M., Salghi R., Lgaz H., Jodeh S., Zougagh M. and Souizi A., Corrosion control of carbon steel in hydrochloric acid by Sulfaguandine: Weight loss, electrochemical and theoretical studies, Der Pharm. Lett., 8 (4), 65-76 (2016).
16. Abou- Elseoud, W. S., Abdel-karim, A. M., Hassan, E. A., & Hassan, M. L. Enzyme-and acid-extracted sugar beet pectin as green corrosion inhibitors for mild steel in hydrochloric acid solution. Carbohydrate Polymer Technologies and Applications, 2, 100072(2021).
17. Fouda A.S., Shalabi K. and Nazeer A.A., Corrosion inhibition of carbon steel by Roselle extract in hydrochloric acid solution: electrochemical and surface study, Res. Chem. Intermed., 41(7), 4833-4850 (2015).
18. Abdel Nazeer A., Shalabi, K., Fouda A.S., Corrosion inhibition of carbon steel by Roselle extract in hydrochloric acid solution: electrochemical and surface study, Res Chem Intermed 41:4833–4850(2015).
19. Chau J.W., Jin M.W., Wea L.L., Chia Y.C., Fen P.C. and Tsui H.T., Protective effect of Hibiscus anthocyanins against tert-butyl hydroperoxide-induced hepatic toxicity in rats, Food Chem. Toxicol. 38 (5), 411 (2000).
20. Kirdpon S., Nakorn S.N. and Kirdpon W., Changes in urinary chemical composition in healthy volunteers after consuming roselle (Hibiscus sabdariffa Linn.) juice, J. Med. Assoc. Thai. 77 (6), 314 (1994).
21. Faraji M.H. and Tarkhani A.H.H., The effect of sour tea (Hibiscus sabdariffa) on essential hypertension, J. Ethnopharmacol. 65 (3), 231-236 (1999).
22. Chen C.C., Hsu J.D., Wang S.F., Chiang H.C., Yang M.Y., Kao E.S., Ho Y.C. and Wang C.J., Hibiscus sabdariffa extract inhibits the development of atherosclerosis in cholesterol-fed rabbits, J. Agric. Food Chem. 51(18), 5472-5477 (2003).
23. Emeka E. Oguzie, Corrosion Inhibitive Effect and Adsorption Behaviour

of Hibiscus Sabdariffa Extract on Mild Steel in Acidic Media, Portugaliae Electrochimica Acta 26, 303-314(2008).

24. Ameer, M.A., Fekry, A.M., Corrosion inhibition by naturally occurring Hibiscus sabdariffa plant extract on a mild steel alloy in HCl solution, Turk J Chem 39: 1078 - 1088(2015).

25. Molina-Ocampo, L.B., Valladares-Cisneros M.G., Gonzalez-Rodriguez J.G., Using Hibiscus Sabdariffa as Corrosin Inhibitor for Al in 0.5 M H2SO4, Int. J. Electrochem. Sci., 10, 388 – 403 (2015) .

26. GaberGh A, Hussein W A, Ahmed A S I, Comparative Study of Electrochemical Corrosion of Novel Designs of 90/10 and 70/30 Copper-Nickel Alloys in Brine Solutions, Egypt. J. Chem. Vol. 63, No. 4, pp. 1527-1540 (2020).

27. Fouda A S, Elmorsi M A, Fayed T, Shaban S M, Azazy O, Corrosion Inhibition of Novel Prepared Cationic Surfactants for API N80 Carbon Steel Pipelines in Oil Industries, Sur. Eng. and App. Electroc., 54, 180–193 (2018).

28. Taha R H, GaberGh A, Mohamed L Z, Ghanem W A, Corrosion Inhibition of Two Schiff Base Complexes on The Mild Steel in 1M HCl Solution, Egypt.J.Chem. Vol. 62, Special Issue (Part 1), pp. 367 - 381 (2019).

29. Aljourani J., RaeissiK.andGolozar M.A., Benzimidazole and its derivatives as corrosion inhibitors for mild steel in 1M HCl solution, Corros. Sci., 51, 1836-1843 (2009).

30. Abdel-Karim, A. M., El-Shamy, A. M., Megahed, M. M., & Kalmouch, A., Evaluation the inhibition efficiency of a new inhibitor on leaded bronze statues from Yemen. Arct J, 71(1), 2-33(2018).

31. Fouda AS, Al-Sarawy A.A, El-Katori E.E, Pyrazolone derivatives as corrosion inhibitors for C-steel in hydrochloric acid solution, Desalination, 201, 1 (2006).

32. Singh, M. R. , Bhrara, K., and Singh G., Port. Electrochim. Acta. 2008, 26, 479-492

33. Gaber Gh A, Maamoun MA, Ghanem WA, Evaluation of the Inhibition Efficiency of a Green Inhibitor on Corrosion of Cu-Ni Alloys in the Marine Application, Key Eng. Mate, 786, 174-194 (2018).

34. Obi-Egbedi N.O.and Obot. I.B.,Corros. Sci., 53, 263-275(2011).

35. Singh, A. K., Quraishi M.A. , The effect of some bis-thiadiazole derivatives on thecorrosion of mild steel in hydrochloric acid, Corros. Sci., 52, 1373- 1385(2010).

36. Belkhaouda M., Bammo L., Salghi R., Zarrouk A., Ebenso E.E., Zarrok H. and Hammouti B., Inedible Avocado Extract: An Efficient Inhibitor of Carbon Steel Corrosion in Hydrochloric AcidInt. J. Electrochem. Sci. 8, 10987- 10999 (2013).

37. Ismail A., Ikram E.H.K. and Nazri H.S.M., Roselle (Hibiscus sabdariffa L.) seeds-nutritional composition, protein quality and health benefits, Food 2 (1), 1-16 (2008).

38. Y. Li, K.L. Chin, F. Malekian, M. Berhane, J. Gager, Circular Ufnr, No. 604 (2005).

39. Singh A.K. and Quraishi M.A., Inhibitive effect of diethylcarbamazine on the corrosion of mild steel in hydrochloric acid, Corros. Sci. 52 (4), 1529-1535 (2010).

40. Umorena, S. A, Obota, I. B., Ebensob, E. E., Obi-Egbedi N.O., Desalination 247, 561 (2009).

41. Popova, A., Sokolova,E. ,Raicheva,S. Christov, M.,Corrosion Science 45 ,33 (2003).